Polish J. Chem., **77**, 283–293 (2003) **INORGANIC CHEMISTRY**

Solution Properties of Cu(II) Complex of a Moderately Hydrophobic Water-Soluble Porphyrin and Investigation of Its Interaction with Human Serum Albumin

by A. Bordbar[1], A. Eslami[2*] and S. Tangestaninejad[1]

[1]*Department of Chemistry, Isfahan University, Isfahan 81744, Iran*
[2]*Department of Chemistry, University of Mazandaran, Babolsar, P.O.Box 47416-1467, Mazandaran, Iran Fax: +98-112-5242029*
E-mail: Eslami@umz.ac.ir and Eslami_a@yahoo.co.uk

(Received October 10th, 2002; revised manuscript December 16th, 2002)

The association behavior of Cu(II) complex of 5,10,15,20-tetrakis(4-N-benzyl-pyridyl)porphyrin (Cu(II)TBzPyP) in aqueous solution at various ionic strength was studied by optical absorption and resonance light scattering (RLS) spectroscopies. The results show that Cu(II)TBzPyP exists as a monomer at low ionic strength and ill-defined aggregates at high ionic strength. The binding of the Cu(II)TBzPyP to human serum albumin (HSA) at 0.005 M phosphate buffer, pH 7.0 and 27°C has been also studied by optical absorption and RLS spectroscopies. The optical absorption spectral patterns of Cu(II)TBzPyP at various concentration of HSA represent two distinct stages in the process of interaction. The existence of an isosbestic point in first titration stage can be related to the equilibrium of free Cu(II)TBzPyP with that of Cu(II)TBzPyP:HSA complex. The aggregation of HSA molecules around porphyrin has occurred in the second titration stage. The analysis of binding process by calculation on absorption data led us to estimate binding constant for formation of HSA:Cu(II)TBzPyP complex. The RLS spectra of Cu(II)TBzPyP at various concentration of HSA do not show any aggregation of Cu(II)TBzPyP in the presence of HSA, which certified the results of UV-Vis studies. The fluorescence emission of HSA chromophore was quenched due to the porphyrin binding. The process of quenching has been analyzed by Stern-Volmer equation. Hence the binding constant of Cu(II)TBzPyP to HSA has also been estimated as the Stern-Volmer quenching constant, which is in good agreement with the result of UV-Vis studies.

Key words: porphyrin, human serum albumin, fluorescence, resonance light scattering

Water-soluble porphyrins and metalloporphyrins are interesting materials in many applied fields [1–4]. For example, as photosensitizer in photodynamic therapy of cancer [1], and as a probe for DNA structure [4]. Biological activity of porphyrins depends strongly on their physico-chemical properties, in particular, self-aggrega-

*Author for correspondence.

tion and affinity to different biological structures. So there is a current interest in exploration of aggregation of water-soluble porphyrins [5–7] and their interaction with DNA and proteins [8–10]. In solution, the planarity and large surface area of the porphyrin macrocycle favor stacking interactions, which lead to large aggregates [11].

The geometry of these aggregates, when no cooperative effects are present, corresponds to homoassociate of low-defined geometry. Detection of porphyrin aggregation is usually performed through their UV/Vis spectra changes, caused by self-aggregation and attributed to several effects. It is generally accepted that a bathochromic or hypsochromic shift of the Soret band (B-band) is a probe of edge-to-edge (J-aggregate) and face-to-face (H-aggregate) homoassociation, respectively [12]. Furthermore, deviation from Beer's law or an increase in the absorption bandwidth is related to the formation of porphyrin stacks without a defined geometry [7,13]. Beside UV/Vis spectra, resonance light scattering (RLS) is recently known as a very sensitive method for monitoring of aggregation of molecules with high absorption in the visible spectral region [14]. The theory behind RLS is based on resonance enhancement of Rayleigh scattering, which arises from electronically coupled arrays of chromophores. Self-assembly of water-soluble porphyrins is highly dependent on the peripheral groups and their charge type [13,15,16]. For example the anionic 5,10,15,20-tetrakis(4-sulfonatophenyl)porphyrin (TPPS4) shows more tendencies for aggregate formation than the cationic 5,10,15,20-tetrakis(4-N-methyl-pyridyl)porphyrin (TMPyP) [5,6,15,17]. The physico-chemical properties of the cationic TMPyP and its metal complexes have been extensively studied [8,13,18]. Neither TMPyP nor its metal derivatives form significant aggregates in aqueous solution even in the presence of inorganic salts that favor self-aggregation of ionic porphyrins. However, binding to DNA or protein may induce the aggregation of such porphyrins [8,19,20]. Among various metalloporphyrins, Cu-complexes have attracted greater attention due to their distinguished photophysical properties and affinity to biological structures [10].

In order to shed more light on the effect of peripheral groups of porphyrin core into aggregation phenomenon and protein binding behavior of metalloporphyrin we have chosen to investigate aggregation of Cu complex of 5,10,15,20-tetrakis(4-N-benzyl-pyridyl)porphyrin (Cu(II)TBzPyP, Scheme 1).

Since human serum albumin (HSA) is known as major plasma of protein and displays effectively drug delivery function [21], the investigation of binding of drug porphyrins with albumin is of interest [20,22,23]. In the present work, we have also studied the interaction of Cu(II)TBzPyP with HSA by UV/Vis, fluorescence and RLS spectroscopy methods. The importance of such studies will appear when we consider this fact that the mechanisms of the biological effects of porphyrin derivatives are different and depend on their peripheral groups. Highly hydrophobic porphyrins can penetrate in the lipid regions of the membranes, moderately hydrophobic ones preferentially distribute into polar parts of the cell, *i.e*. protein rich membrane domains [24], while highly polar species exclusively partition in the aqueous compartment, their binding to cellular membrane being poor [25]. Regarding to the fact that the

Scheme 1

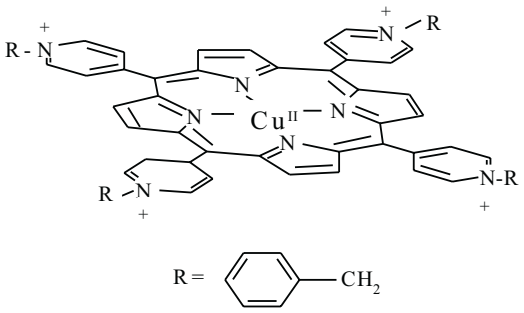

Cu(II)TBzPyP

Cu(II)TBzPyP has more hydrophobic property compared to previously reported water-soluble porphyrins we may consider it as promising compound for clinical applications.

EXPERIMENTAL

Materials and methods: Tetra(4-pyridyl)porphyrin (TPyP) was obtained from Aldrich and used as received. TBzPyP was prepared from its precursor, TPyP, by reaction with benzyl bromide in DMF. The copper(II) derivative of TBzPyP was prepared, purified and converted to its chloride form by a slightly modified published procedure [26]. HSA, free acid free fraction V (97–98%), was obtained from Sigma and used as received. Absorption spectra were recorded on a Shimadzu UV-2100 double beam spectrometer with a thermostat cell compartment. Fluorescence and resonance light scattering experiments were performed with a Perkin Elmer LS 50B luminescence spectrometer. In all experiments, the porphyrin and HSA solutions were freshly prepared before spectral analysis and were protected from direct sunlight and fluorescent light until they were inserted into the cell compartments. To observe the salt effect on the porphyrin absorption and RLS spectra the titration were made by addition of aliquots of the NaCl solution into a cuvette containing the porphyrin solution of appropriate concentration. The titration of porphyrin solution in function of HSA concentration was performed at pH 7. Measurments were performed in 0.005 phosphate buffer. The scattered light intensity (SLI) was monitored using the right-angle geometry in the synchronized-scanning regime of the excitation and emission monochromator the region from 300 to 600 nm. The experimental light scattering spectra were corrected taking into account the solution optical absorption and the instrument sensitivity dependence on the wavelength as described elsewhere [27]. In these experiments the bandwidth for excitation and emission was 3 nm. The quenching of HSA fluorescence by porphyrin was monitored using excitation in the region of absorption maximum at 280 nm and bandwidth of 5 nm for both excitation and emission slits.

RESULTS AND DISCUSSION

Solution properties of Cu(II)TBzPyP: In order to identify the solution properties of Cu(II)TBzPyP, we employed UV/Vis and resonance light scattering techniques. Optical absorption spectrum of Cu(II)TBzPyP shows two overlapping Q-bands with

maximum at 551 nm, which is a characteristic of D_{4h} symmetry of porphyrin central ring. The maximum of the Soret band appears at 429.3 nm. The molar absorptivities of the Soret band and Q-band are 1.55×10^5 and 1.55×10^4 M^{-1} cm^{-1}, respectively. The Soret band maximum of Cu(II)TBzPyP obeys Beer's law over an extended concentration range between 5.43×10^{-7} to 1.2×10^{-4} in phosphate buffer 0.005 M, pH 7.0. From this observation we can conclude that Cu(II)TBzPyP does not show concentration dependent aggregation in this concentration range.

Effects of inorganic salts: It is well known that self-association of the water-soluble porphyrin is facilitated by inorganic salts [5,13,27]. The effect of NaCl on the absorption spectrum of Cu(II)TBzPyP (4.4×10^{-6} M) in water is shown in Figure 1.

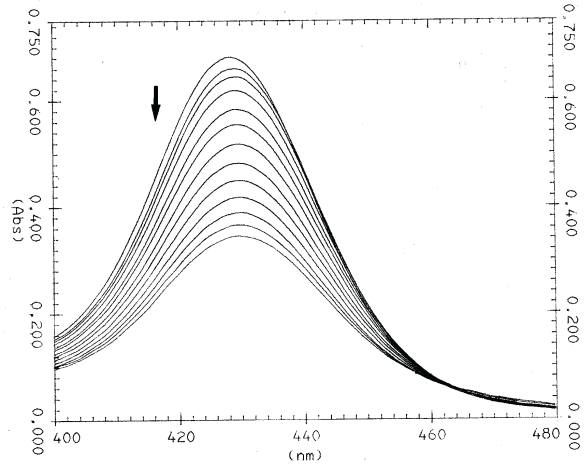

Figure 1. Absorption spectral changes of Cu(II)TBzPyP complex upon addition of NaCl (0, 0.103, 0.202, 0.385, 0.631, 0.848, 1.099, 1.036, 1.59, 1.782, 1.948, 2.093 and 2.220 M) in water (pH 6.7) at 27°C. The arrow show the increasing of NaCl concentration.

As the concentration of NaCl increases, the absorbance at all of the spectral regions has been decreased and the Soret band becomes very broad with a red shift. The data concerning these spectral changes are presented in Table 1.

Although, the absorption spectrum of Cu(II)TBzPyP shows a significant electrolyte effect, but no new band appears even in high salt concentration. This result means that Cu(II)TBzPyP does not form well-defined aggregates (*i.e.* H or J types) in the presence of a salt [6]. Thus, these spectral changes can be attributed to the formation of extended ill-defined aggregates. From this observation, it also can be concluded that Cu(II)TBzPyP lacks axial ligands.

Table 1. UV/Vis spectral changes of a water solution of Cu(II)TBzPyP (4.4×10^{-6} M) upon increasing of NaCl concentration.

[NaCl], M	λ_{max} (nm)	Abs (max)	$W_{1/2}$ (nm)[a]
0	429.3	0.682	32.3
0.103	430.1	0.660	32.6
0.202	430.2	0.644	32.6
0.385	430.3	0.619	32.8
0.631	430.3	0.583	33
0.848	430.4	0.554	33.4
1.099	430.4	0.554	33.7
1.365	430.5	0.482	34
1.590	430.7	0.449	34.4
1.780	430.8	0.418	35.1
1.948	431.0	0.389	35.1
2.093	431.4	0.369	35.6
2.220	431.5	0.354	35.8

[a]Half-width of the Soret band.

Figure 2 demonstrates the RLS profile of the Cu(II)TBzPyP solutions in various concentration of NaCl, which are corrected taking into account both spectrofluorimeter sensitivity on λ and NaCl effect.

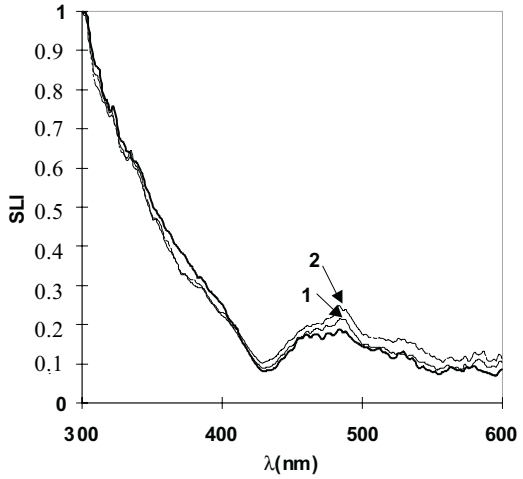

Figure 2. Resonance light scattering spectra of Cu(II)TBzPyP (1.39×10^{-6} M) at various concentration of NaCl: 0 (solid line), 1.146 (1) and 2.200 M (2).

With respect to this figure the SLI spectra of Cu(II)TBzPyP slightly increase upon increasing of NaCl and analogues to other porphyrin [6,28], SLI (Scattered Light Intensity) in Soret region is small. The formation of extended aggregates is usually accompanied by significant increasing of the RLS signal near to Soret band region (*i.e*. Q-band's region). This effect has not been observed in RLS profile of the Cu(II)TBzPyP. It seems that this result is in contrast with the results of UV-Vis studies. However, this observation can be attributed to the lacking of porphyrin chromo-

phore coupling in the aggregates, which reduces the enhancement of light scattering due to aggregation. The similar observation has been reported for Cu-derivatives of other porphyrins [6,29], which certified our interpretation and assigning the special role of copper in this process.

Binding of Cu(II)TBzPyP to HSA. Optical absorption: Refereing to our previous discussion we can conclude that, in homogeneous aqueous solution at low ionic strength, Cu(II)TBzPyP exists mainly as monomer. So, we conducted the titration of porphyrin solution at fixed concentration of Cu(II)TBzPyP and varying [HSA] at pH 7.0 and 0.005 M phosphate buffer, as a low ionic strength medium. Figure 3a shows a representative titration spectrum of Cu(II)TBzPyP upon increasing concentration of HSA. The addition of HSA changes the position, width and intensity of Soret band of Cu(II)TBzPyP. These spectral changes can be treated as two consecutively distinct changes. At initial HSA additions, [HSA]/[Cu(II)TBzPyP] < 1.3, the intensity of the Soret band decreases and titration spectra are accompanied by the appearance of an isosbestic point at 446 nm, shown with one asterisk in Figure 3a (Stage I). Higher addition of HSA causes the disappearance of the isosbestic point and the increasing the Soret band intensity. This stage of titration is not accompanied with any isosbestic point. The well-defined end point has not been observed for stage II, which can be attributed to distribution of porphyrin into various HSA aggregates [23].

Since the spectrum of free Cu(II)TBzPyP passes through this isosbestic point, the contribution of free Cu(II)TBzPyP to first equilibrium should be taken into account. The first isosbestic point appears at a molar ratio [HSA]/[Cu(II)TBzPyP] < 1.3, so it seems that the major component is free porphyrin in equilibrium with a 1:1 conjugate (*i.e.* Cu(II)TBzPyP…HSA, stage I):

$$\text{Cu(II)TBzPyP} + \text{HSA} \longleftrightarrow \text{Cu(II)TBzPyP...HSA} \qquad (1)$$

The formation of protein aggregates around porphyrin has also been noted in some earlier reports [23,30]. It is reasonable to assume that HSA aggregates with different aggregation number exist at higher concentration of HSA. Therefore, the spectral changes in stage II could be due to distribution of Cu(II)TBzPyP within many different HSA aggregates.

The analysis of the optical absorption data: Based on our earlier results [20,31], it is possible to calculate the average number of bound porphyrin to one molecule of HSA(ν), by analysis of absorption band data. Regarding equilibrium (1), we can defined ν as:

$$\nu = \frac{[\text{Cu(II)TBzPyP}\ldots\text{HSA}]}{[\text{HSA}]_{\text{total}}} \qquad (2)$$

By such calculation the Scatchard plot for titration stage I has been constructed and shown in Figure 3b. The high correlation coefficient of this linear plot and X-inter-

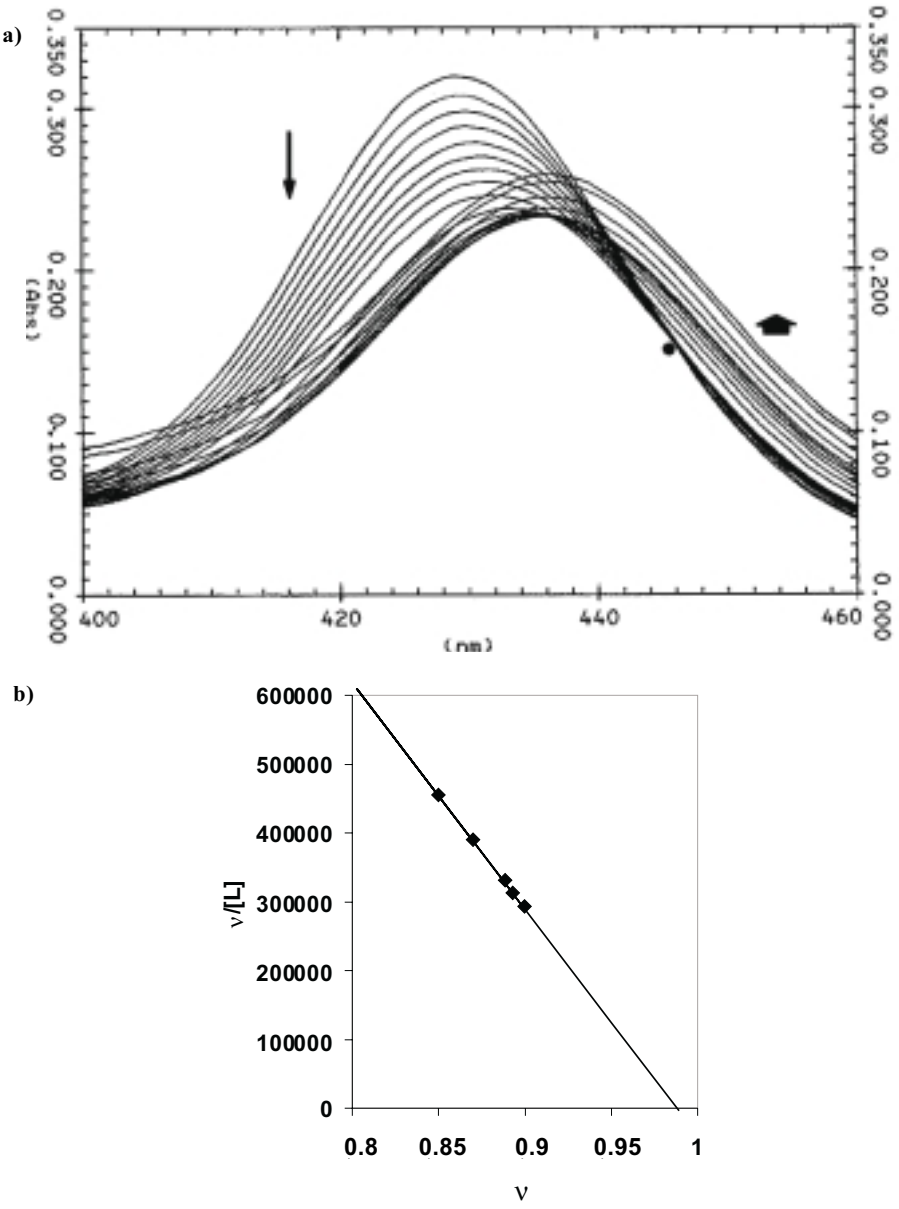

Figure 3. a) The overall absorption spectral changes of Cu(II)TBzPyP (2.06×10^{-6} M) in 0.005 M phosphate buffer at pH 7.0 and 27°C upon addition of HSA from 0 to 4.30×10^{-6} M. The spectra of first titration stage appeared with one isosbestic point shown with one asterisk. **b**) The Scatchard plot for first titration stage, [L] = $[Cu(II)TBzPyP]_{free}$.

cept near to one confirmed the formation of 1:1 complex and our analyzing method. The value of 3.3×10^{6} M^{-1} was obtained for formation constant of Cu(II)TBzPyP:HSA complex.

Light scattering experiments: Figure 4 demonstrates the relative SLI profiles of the Cu(II)TBzPyP solutions in the presence of different HSA concentrations. The SLI in the region from 450 to 500 nm slightly changes upon the HSA addition. In fact, this represents that the addition of HSA to the Cu(II)TBzPyP solutions has little effect on the aggregation state of this porphyrin. This confirmed the UV-Vis results, corresponds to aggregation of HSA around porphyrin.

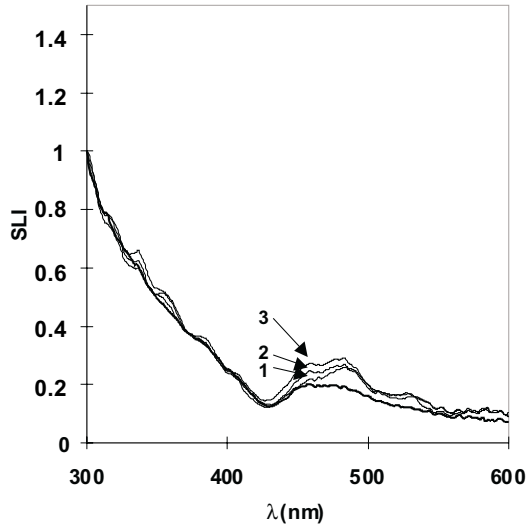

Figure 4. Resonance light scattering spectra of Cu(II)TBzPyP (8.77×10^{-7} M) in 0.005 phosphate buffer at pH 7.0 and 27°C upon addition of HSA: 0 (solid line), 4.89×10^{-8} M (1), 9.64×10^{-8} M (2), and 1.42×10^{-7} M (3).

Fluorescence quenching of HSA by Cu(II)TBzPyP: The addition of Cu(II)TBzPyP to HSA solution does not have any significant influence on the optical absorption spectra of HSA. However, the stepwise addition of Cu(II)TBzPyP to HSA solution resulted in a progressive quenching of the fluorescence emission, shown in Figure 5a. For fluorescence quenching of HSA a Stern-Volmer relationship can be applied:

$$\frac{F_{max}}{F} = 1 + K_{SV}[\text{Cu(II)TBzPyP}] \qquad (3)$$

where F_{max} and F are the fluorescence intensities in the absence and presence of quencher, *i.e*. Cu(II)TBzPyP, respectively. K_{SV} is Stern-Volmer constant. The linear Stern-Volmer plot, shown in Figure 5b, indicates that (2) is applicable for present system. These titration experiments were conducted at a $[HSA]_0/[Cu(II)TBzPyP]$ molar ratio of 4.44 to 0.351, which approximately corresponds to first titration stage in optical absorption measurement. So, the Stern-Volmer constant could be approximately regarded as K^I,which is 3.4×10^5 M^{-1}.

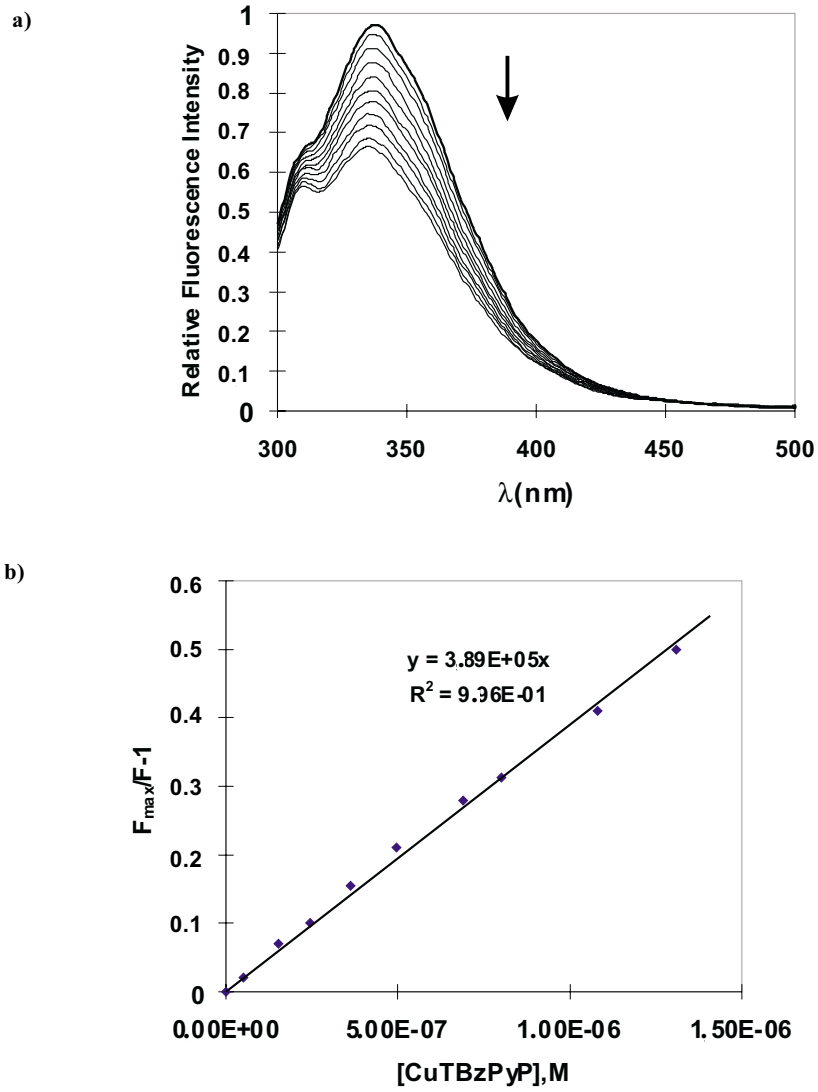

Figure 5. a) Corrected emission spectra of HSA, 2 ml (1.08×10^{-6} M) plus added Cu(II)TBzPyP (3.51×10^{-6} M) in 0.005 M phosphate buffer pH 7 μl Cu(II)TBzPyP solution added from 0, 60, 90, 160, 150, 160, 150, 10, 150, 150 and 150. The arrow shows the increasing of Cu(II)TBzPyP concentration. **b**) Stren-Volmer plot for the fluorescence quenching of HSA by Cu(II)TBzPyP.

CONCLUSIONS

Cu(II)TBzPyP as a metalloporphyrin can exhibit distinguished photophysical properties and due to their benzyl peripheral groups has a considerable hydrophobic property that increases its ability for penetration in the lipid region of the biological

membranes. The pattern of optical absorption spectrum of this porphyrin represents D_{4h} symmetry of porphyrin central ring. The Soret band maximum of Cu(II)TBzPyP obeys Beer's law over an extended concentration range between 5.43×10^{-7} -1.2×10^{-4} M, which represents that this porphyrin does not show concentration dependent aggregation. As like as many other porphyrins, inorganic salts facilities the self-association of Cu(II)TBzPyP. However, the effect of salt on absorption spectrum of Cu(II)TBzPyP does not induce the formation of well-defined aggregates (*i.e*. J or H types). The formation of ill-defined aggregates at high concentration of salt has been concluded from RLS spectra. This fact is in contrast with the behavior of most other porphyrins that their association is usually accompanied by significant increasing of RLS signal near to Soret region. This behavior can be related to the spectral role of Cu in the lacking of porphyrin chromophore coupling in the aggregates, which is responsible for no enhancement of scattered light.

Binding studies of Cu(II)TBzPyP with HSA represent the existence of a specific site on HSA for binding of Cu(II)TBzPyP. The occupation of this site at low molar ratio of [HSA]/[Cu(II)TBzPyP] (< 1.3) causes the formation of Cu(II)TBzPyP:HSA complex whose formation constant can be estimated by analysis of absorption data. However, at higher concentration of HSA, the aggregation of HSA around porphyrin is observed.

Acknowledgments

Financial supports from research councils of Mazandaran and Isfahan Universities are gratefully acknowledged.

REFERENCES

1. Bonnett R., *Chem. Soc. Rev.*, 19 (1995).
2. Lewis D.E., Utrecht R.E., Judy M.M., Matheus L.J. and Chanh T.C., *Spectrum*, **6**, 8 (1993).
3. Cannon J.B., *J. Pharm. Res.*, **82**, 435 (1993).
4. Pasternack R.F. and Gibbs E., "*Metal-DNA Chemistry*", ACS symposium Series 402, ed. by T.D. Tullius, American Chemical Society, Washington (1989) pp. 57–43.
5. Kano K., Minanizono H., Kitac T. and Negi S., *J. Phys. Chem*., **101**, 6118 (1997).
6. Pasternack R.F., Schaefer K.F. and Hambright P., *Inorg. Chem.*, **33**, 2062 (1994).
7. Ribo J.M., Crasts J., Farrera J.A. and Valero M.L., *J. Chem. Soc., Chem. Comm*., 681 (1994).
8. Gandini S.C.M., Yushmanov V.E., Perssui J.R., Tabak M. and Borissevitch I.E., *J. Inorg. Biochem*., **73**, 35 (1999).
9. Pasternack R.F., Giannetto A., Pagano P. and Gibbes E.J., *J. Am. Chem. Soc*., **113**, 7799 (1991).
10. McMillon D.K. and McNett K.M., *Chem. Rev.*, **98**, 1201 (1998).
11. Hunter C.A. and Sanders J.K.M., *J. Am. Chem. Soc*., **112**, 5525 (1990).
12. Barber D.C., Feity-Besston R.A. and Whitten D.G., *J. Phys. Chem*., **95**, 4074 (1991).
13. Pasternack R.F., Huber P.R., Boyd P., Engasser G., Francesconi L., Gibbs E., Fasella P., Ventro G.C. and Hinds L.de.C., *J. Am. Chem. Soc*., **94**, 4511 (1972).
14. Pasternack R.F. and Collings P.J., *Science*, **269**, 935 (1995).
15. Rubires R., Crusats J., El-Hachemi Z., Farrera J.A. and Ribo J.M., *New J. Chem*., 189 (1999).
16. Jin R.H., Aoki S. and Shima K., *Chem. Comm*., 1939 (1996).
17. Huany L.Z., Li Y.F., Li N., Li K.A. and Tang S.Y., *Bull. Chem. Soc. Jpn*., **71**, 1791 (1998).

18. Bute K. and Nakamoto K., *Inorg. Chim. Acta*, **167**, 97 (1990).
19. Gandini S.C.M., Borissevitch I.E., Perssui J.R., Imasato H. and Tabak M., *J. Luminescence*, **78**, 53 (1998).
20. Bordbar A.K., Tangestaninejad S. and Eslami A., *J. Biochem. Mol. Biol. Biophys*., **5**, 143 (2001).
21. Carter D.C. and Ho J., *Advances in Protein Chemistry*, **45**, 53 (1994).
22. Tominaga T.T., Yushmanov V.G., Borissevitch I.E., Imasato H. and Tabak M., *J. Inorg. Biochem.*, **65**, 235 (1997).
23. Borissevitch I.E., Tominaga T.T., Imasato H. and Tabak M., *J. Luminescence*, **69**, 65 (1996).
24. Ricchelli F., Gobbo S., Jori G., Moreno V., Vinzens F. and Salet C., *Photochem. Photobiol.*, **58**, 53 (1993).
25. Ricchelli F. and Jori G., *Photochem. Photobiol*., **44**, 151 (1986).
26. Pasternack R.F., Gibbs E.J. and Villafranca J.J., *Biochem.,* **22**, 2406 (1983).
27. Borissevitch I.E., Tominaga T.T., Imasato H. and Tabak M., *Anal. Chim. Acta*, **343**, 53 (1997).
28. Pasternack R.F., Spiro E.G. and Teach M., *J. Inorg. Nucl. Chem*., **36**, 599 (1974).
29. Kano K., Fukuda K., Wakami H., Nishiyaba R. and Pasternack R.F., *J. Am. Chem. Soc*., **122**, 7494 (2000).
30. Kano K., Takei M. and Hashimato V., *J. Phys. Chem*., **94**, 2181 (1990).
31. Bordbar A.K., Eslami A. and Tangestaninejad S., *J. Porphyrins and Phthalocyanines*, **6**, 225 (2002).